Pergamon

Geochimica et Cosmochimica Acta, Vol. 68, No. 7, pp. 1677–1689, 2004
Copyright © 2004 Elsevier Ltd
Printed in the USA. All rights reserved
0016-7037/04 $30.00 + .00

doi:10.1016/j.gca.2003.10.004

An experimental study of the formation of metallic iron in chondrules

Bosmat A. Cohen* and Roger H. Hewins
Geological Sciences, Rutgers University, 610 Taylor Road, Piscataway, NJ 08854, USA

(*Received February* 20, 2003; *accepted in revised form October* 8, 2003)

Abstract—The abundance of metallic iron is highly variable in different kinds of chondrites. The precise mechanism by which metal fractionation occurred and its place in time relative to chondrule formation are unknown. As metallic iron is abundant in most Type I (FeO-poor) chondrules, determining under what conditions metal could form in chondrules is of great interest. Assuming chondrules were formed from low temperature nebular condensate, we heated an anhydrous CI-like material at 1580°C in conditions similar to those of the canonical nebula ($P_{H2} = 1.3 \times 10^{-5}$ atm). We reproduced many of the characteristics of Type IA and IIA chondrules but none of them contained any iron metal. In these experiments FeO was abundant in charges that were heated for as long as 6 h. At a lower temperature, 1350°C, dendritic/cellular metal crystallized from Fe-FeS melts during the evaporation of S. However, the silicate portion consisted of many relict grains and vesicles, not typical of chondrules.

Evaporation experiments conducted at $P_{H2} = 1$ atm and 1565°C produced charges containing metallic iron both as melt droplets and inclusions in olivine, similar to those found in chondrules. Formation of iron in these experiments was primarily the result of desulfurization of FeS. With long heating times Fe° was lost by evaporation. Apart from some reduction of FeO by kerogen to make metal inclusions within olivine grains, reduction of FeO to make Fe° in these charges was not observed.

This study shows that under canonical nebular conditions FeS and iron-metal are extremely volatile so that metal-rich Type I chondrules could not form by melting "CI." Under these conditions FeO is lost predominantly by hydrogen stripping and, due to the relative low abundance of hydrogen at low pressures, remains in the melt for as long as 6 h. Conversely, at higher total pressures (1-atm H_2) iron metal (produced mainly by the desulfurization of troilite) is less volatile and remains in the melt for longer times (at least 6 h). In addition, due to elevated pressures of hydrogen, FeO is stripped away much faster. These results suggest that chondrule formation occurred in environments with elevated pressures relative to the canonical nebula for iron metal to be present. *Copyright © 2004 Elsevier Ltd*

1. INTRODUCTION

Chondrules, the principal constituent in chondritic meteorites, are crystalline silicate droplets. Type I and Type II chondrules contain FeO-poor and FeO-rich silicates respectively (McSween, 1977; Scott and Taylor, 1983; Jones and Scott, 1989). The main opaque phases are FeNi-metal in Type chondrules and troilite and pentlandite in Type II. Metallic iron-nickel in Type I chondrules occurs in several forms. In some Type I chondrules, metal is distributed throughout the silicates, especially in the mesostasis, and is evenly distributed throughout the chondrules from core to rim (Jones and Scott, 1989). In others it forms round blebs, several tens of microns across usually situated close to the center of the chondrule or in smaller beads around its rim. The metal blebs are larger in coarser grained chondrules, suggesting coalescence of metal droplets in more extensively melted chondrules (Zanda et al., 1993; McCoy et al., 1999; Zanda et al., 2002). Metallic iron also appears in chondrules as fine dusty speckles in relict olivine grains commonly known as "dusty olivine." These grains are commonly forsteritic and contain micron-size blebs of Ni-poor Fe-metal (Nagahara, 1981; Rambaldi, 1981).

There are several possible origins for iron-metal in chondrules. Iron may have been present in the precursors of chondrules (either as iron-metal or FeS), it may be the product of FeO-reduction in the presence of a reducing agent (Connolly et al., 2001), or it may have originated by recondensation of Fe° previously lost from chondrule melts. In some chondrites, chondrules and iron metal were suggested to have formed by direct condensation from the solar nebula (e.g., Krot et al., 2000).

Chondritic meteorites bear evidence of vast nebular fractionations, of volatile elements from refractory, and of silicate phases from metallic (e.g., Larimer and Wasson, 1988). Chondrule formation is associated with heating episodes during which volatile loss would have been unavoidable for canonical nebular conditions (Yu and Hewins, 1998). Although Grossman (1996) disputes the possibility that major fractionations occurred as a result of chondrule formation, others (e.g., Sears et al., 1992; Scott and Haack, 1993; Scott et al., 1996) have suggested separation of chondrules and metal grains with different aerodynamic properties to explain differences in chondrite bulk compositions. Grossman and Wasson (1985) demonstrated that metal droplets could have separated from liquid chondrules, and it is possible that chondrule formation, in which FeO-silicates are melted under reducing conditions, could give rise to metal-silicate fractionation in chondrites (Haack and Scott, 1993). The conditions of formation of chondritic metal are therefore of great interest.

Several experiments have successfully produced iron-metal in chondrule-like compositions (e.g., Tsuchiyama and Miyamoto, 1984; Connolly et al., 1994; Libourel and Chaussidon, 1995), but none of them were conducted under the conditions

* Author to whom correspondence should be addressed (bosmat@rci.rutgers.edu).

Table 1. Starting material (based on Anders and Grevesse, 1989) from DCP analysis plus FeS and kerogen as weighed (in wt%).

Oxide	Starting material
SiO_2	30.69
Al_2O_3	2.56
TiO_2	0.06
FeO	18.21
MnO	0.21
MgO	21.35
CaO	1.65
Na_2O	1.08
K_2O	0.14
FeS	20.27
C	3.77
Total	100

of low hydrogen pressure in which chondrules are believed to have formed. Any study of iron metal aimed at understanding chondrule origins must clearly be in conjunction with studying their silicates, and considering possible effects of evaporation and reduction of FeO in them. In this study we conducted several sets of experiments to restrict the physical conditions in which metal-bearing chondrules are generated by melting low temperature nebular condensates (since S is found in chondrules). In these experiments we used a CI-like starting material composed of phases stable in the nebula at 500 K (Wood and Hashimoto, 1993). It contained troilite and kerogen to examine the possible formation of metallic iron by the reduction of FeO in silicates and/or desulfurization of FeS, and its apparent stability under three different sets of conditions. Conditions were (1) low pressure (1.3×10^{-5} atm H_2) and typical high chondrule-forming temperature (1580°C) (2) low pressure (1.3×10^{-5} atm H_2) and low temperature (1350°C) and (3) high pressure (1 atm H_2) and high temperature (1565°C).

2. EXPERIMENTAL METHODS

Experiments were conducted in two Del-Tech vertical muffle tube furnaces at the Department of Geological Sciences at Rutgers University. A low-pressure furnace with T_{max} = 1580°C and a 1-atm furnace with T_{max} = 1565°C. The starting material was designed to match CI elemental abundance (Anders and Grevesse, 1989) using the phases stable at 500 K under canonical nebular conditions (Wood and Hashimoto, 1993). The starting material was a mineral mixture of 50 wt% Kiglapait olivine (Fo_{66}), 10 wt% San Carlos olivine (Fo_{88}), the two together giving the abundance and composition of the nebular olivine, equal amounts (8 wt%) of diopside and plagioclase, 20.3 wt% Canyon Diablo troilite (63.4 wt% Fe and 36.5 wt% S) or terrestrial pyrrhotite (61.8 wt% Fe and 38.3 wt% S) and 3.8 wt% Sarro-Lorraine kerogen (composed of 77.3% C, 12.4% O, 4.8% H, 1.3% N, 0.8% S, 0.1% Fe and 0.8 loss on ignition). The oxide composition is shown in Table 1. The calculated liquidus temperature of the silicate portion was 1633 ± 30°C (Herzberg, 1979). Minerals were crushed into a 45–63 μm grain sized powder. In all runs, pressed pellets (~50 mg) were hung on an iron-plated rhenium wire. Temperatures were measured using a Type S thermocouple calibrated against the melting point of palladium (1544°C) or gold (1064°C).

Bulk chemistry analyses of the experimental charges were performed by Direct Current Plasma Atomic Emission Spectrometry (DCP-AES). Charges, crushed into 200 mesh powders, were mixed with $LiBO_2$, fluxed and dissolved in HNO_3 solution. The solutions were run on the DCP-AES together with USGS standards such as BHVO-1, BIR-1 and PCC-1 and working standards. Standards were used for both calibration and as control samples.

Analyses of the olivine crystals and mesostasis were performed on a JEOL 8600 microprobe using an accelerating potential of 20 kV, a beam current of 15–20 nA. Counting times varied between 20–40 s. Sodium and potassium were analyzed first with shorter counting times to minimize loss during analyses. Mesostasis analyses were performed using a 5μm-rastered beam.

2.1. Low P and High T Experiments

These experiments were conducted at a temperature of 1580°C in the low-pressure furnace, the design of which has been described in Yu et al. (2003). After the pressure, monitored by an HPS 941 cold cathode pressure gauge, reached 1×10^{-4} torr (1.31×10^{-7} atm), hydrogen gas was introduced into the furnace to a total pressure of 1×10^{-2} torr (1.31×10^{-5} atm).

The oxygen fugacity in the vacuum furnace was calculated using the H_2O/H_2 ratio in the furnace. Air to hydrogen ratio, based on the P_{vacuum}/P_{H2}, was 1/100. The oxygen to hydrogen ratio was therefore 1/500, for which the H_2O/H_2 ratio would be 1/250 (upper limit). The vol% of H_2O in (H_2+H_2O) is ~0.4. Based on calculations by Deines et al. (1974), an H_2O volume percent of 0.4 at 1580°C correlates with an oxygen fugacity log $fO_2 = -11.8$ atm. For calculating the IW buffer at 1853 K and P of 1.31×10^{-5} atm we used the following equation (Darken and Gurry, 1945; Eugster and Wones, 1962):

$$\log fO_2 = -27215/T + 6.57 + \{0.055(P - 1)/T\}$$

The IW buffer at the experiment conditions is at log $fO_2 = -8.12$ atm. The oxygen fugacity during our experiments is therefore at most 3.7 below the IW buffer, and fell during experiments because of continued flow of hydrogen.

Runs were conducted under continuous hydrogen flow and pumping. Experimental runs were 1, 2, 4, 6, 12 and 18 h long and were quenched in the furnace by elevating the sample into the antechamber (≈10000°C/h). In these experiments the sulfide in the starting material was Canyon Diablo troilite.

2.2. Low P and Low T Experiments

These experiments were conducted at 1350°C in the low-pressure furnace. Hydrogen pressure in these runs was similar to the one in §2.1. However, due to the lower temperature the initial oxygen fugacity in these experiments is slightly lower and was calculated to at most 4.8 log units below the IW buffer. The oxygen fugacity was calculated as in §2.1 except for 1350°C. Experimental charges were heated isothermally for 2, 10 and 30 min at a time and were quenched in the furnace by elevating the sample into the antechamber (~10,000°C/h). The sulfide in the starting material was Canyon Diablo troilite.

2.3. High P and High T Experiments

These experiments were conducted at 1-atm pressure and a temperature of 1565°C. A mixture of H_2-CO_2 yielded an oxygen fugacity, measured with a zirconia cell (Nafziger et al., 1971; Huebner, 1987), of 3 log units below the IW buffer curve. Samples were heated for 1, 2, 4, 6, 12 and 18 h. At the end of each run the sample was pulled out of the furnace and immediately quenched in water. In these experiments the sulfide in the starting material was terrestrial pyrrhotite.

3. RESULTS

3.1. Low P and High T Experiments

The experimental charges produced in these experiments contained only olivine and mesostasis (for more texture and composition details, see Cohen et al., 2000). Chemical analyses have shown that FeS, and alkalis were lost within the first hour. During the first 6 h of heating the major component being lost was FeO and after 12–18 h it became SiO_2. Minor amounts of MgO were lost as the residues attained the composition of an Al-enriched Type IA chondrule (Jones and Scott, 1989).

The concentration of FeO in the bulk composition gradually

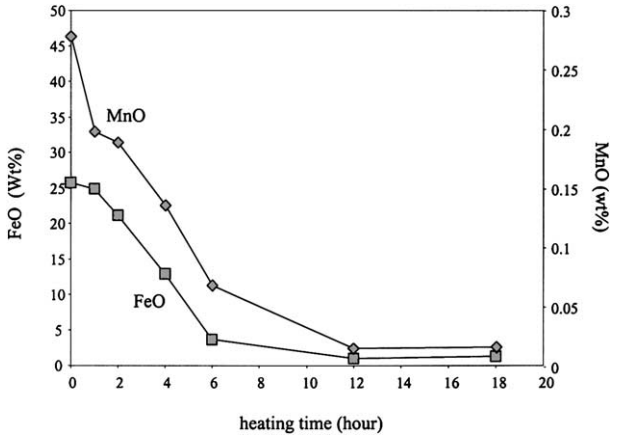

Fig. 1. The bulk concentration of FeO and MnO (wt%) versus heating times (hours) in the charges produced at 1580°C in H_2 at 1.3×10^{-5} atm.

decreased from ~25 wt% in the starting material to less than 5 wt% after ~6 h of evaporation (Fig. 1). The evaporation of FeO from our charges is consistent with hydrogen reaction rather than free evaporation (Nagahara and Ozawa, 1996; Tsuchiyama, 1999) and may have occurred in several ways. Iron oxide could have been lost in a two-step mechanism, first reduction to Fe° in the melt and later evaporation of Fe°:

$$FeO_{(l,s)} + H_2 \rightarrow Fe_{(l)} + H_2O \quad (1)$$

$$Fe_{(l)} \rightarrow Fe_{(g)} \quad (2)$$

Otherwise, FeO could have been stripped from the charges by hydrogen molecules (hydrogen stripping), following the reaction:

$$FeO_{(l)} + H_2 \rightarrow Fe_{(g)} + H_2O \quad (3)$$

To distinguish between the two mechanisms for FeO-loss we used the dichotomy in the behavior of FeO and MnO under reducing conditions. In melts of chondrule composition, the volatility of MnO is similar to that of FeO (Cohen et al., 2000), but under reducing conditions Fe enters the metal phase while Mn remains in the silicate. In our experiments, the bulk concentrations of FeO and MnO (in wt%) decrease following a similar pattern as heating times increase (Fig. 1). For this reason MnO is lost solely by hydrogen stripping (similar to Eqn. 3). The contents of FeO and MnO in the olivine and mesostasis are presented in Table 2. A comparable decrease in the content of FeO and MnO in the olivine and the mesostasis is observed as well (Fig. 2). The trends shown in Figures 1 and 2 firmly support FeO-loss by hydrogen stripping rather than the two step mechanism of reduction to Fe-metal followed by evaporation. It is important to note that comparison between FeO and MnO contents as a proxy for inferring FeO reduction can only be possible if the evaporation rate of MnO is different than the reduction rate of FeO.

The amount of FeO (in moles) lost in each experiment was calculated on the basis of the initial and final weights of the different charges and their bulk chemistries. Dividing the difference in FeO loss between two successive runs by the time difference and the surface area of the charge gives evaporation rates in hydrogen. Evaporation rates varied between 3.94×10^{-6} and 1.17×10^{-8} mole/cm^2/s for 0–1 to 12–18 h, respectively (solid circles in Fig. 3).Wang et al. (1994) used data from Barin (1989) to calculate theoretical evaporation rates for a number of reactions involving the evaporation of $Fe_{(g)}$ from pure phases as a function of temperature (Fig. 3). The evaporation rates obtained in this study are about an order of magnitude higher than the theoretical values for $FeO_{(l)} \rightarrow Fe_{(g)} + \frac{1}{2} O_{2(g)}$. These results are related to the presence of hydrogen and to the fact that FeO is predominantly lost by hydrogen stripping (Eqn. 3). The effect of the presence of

Table 2. Final compositions of olivine and mesostasis (wt%) in the experimental charges performed at $P_{H2} = 1.31 \times 10^{-5}$ atm and 1580°C.

Oxide (wt%)	1 h	s.d.[a]	2 h	4 h	6 h	12 h	18 h
Olivine							
No. of analyses	19		16	21	17	15	16
SiO_2	38.48	0.50	39.47	40.68	41.99	42.66	42.55
Al_2O_3	0.02	0.051	0.03	0.02	0.03	0.07	0.32
TiO_2	0.03	0.019	0.00	0.01	0.01	0.01	0.02
FeO	16.79	0.63	15.81	10.65	4.73	0.60	0.33
MnO	0.21	0.019	0.05	0.07	0.06	0.01	0.00
MgO	43.56	0.63	44.19	47.95	52.84	55.62	55.51
CaO	0.13	0.066	0.14	0.09	0.12	0.25	0.64
Total	99.21		99.69	99.47	99.77	99.23	99.38
Fo content	82.22		83.28	88.92	95.22	99.40	99.66
Mesostasis							
No. of analyses	13		14	11	12	14	10
SiO_2	44.69	1.51	45.63	48.98	52.42	45.50	37.62
Al_2O_3	5.46	0.044	5.44	4.84	7.02	14.26	17.18
TiO_2	0.11	1.75	0.11	0.10	0.15	0.29	0.42
FeO	25.95	0.92	21.74	13.19	2.20	0.11	0.02
MnO	0.24	0.027	0.20	0.14	0.06	0.01	0.00
MgO	19.64	6.00	21.82	28.07	31.21	29.15	26.69
CaO	4.08	1.97	4.03	3.96	5.84	10.96	17.90
Total	100.14		99.00	99.32	98.92	100.31	99.85

[a] Averaged standard deviations.

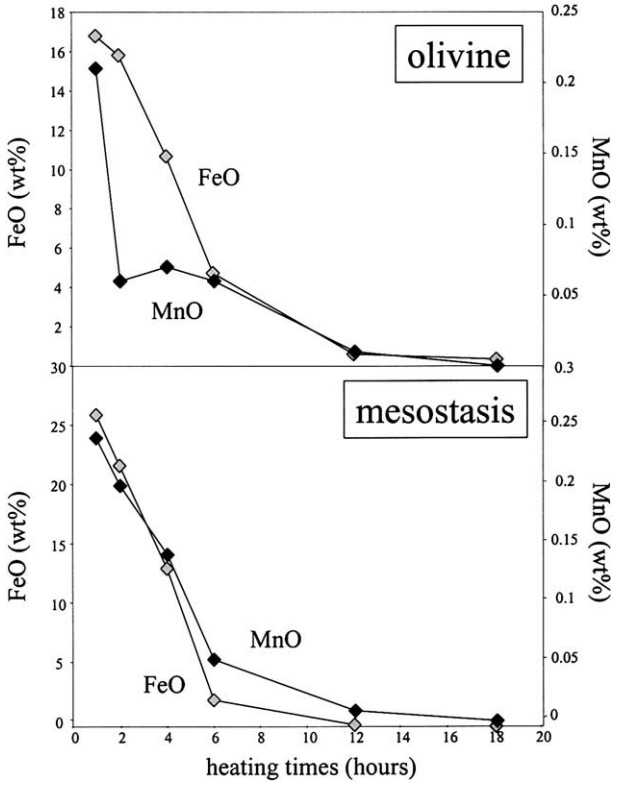

Fig. 2. The concentration of FeO and MnO (wt%) in the olivine and the mesostasis phases versus heating times (hours) in the charges produced at 1580°C in H_2 at 1.3×10^{-5} atm.

hydrogen on the evaporation rate of FeO is further demonstrated when compared with results by Wang et al. (2001) who have conducted vacuum evaporation experiments at 1800°C using a similar composition but with residual air as the ambient gas. The evaporation rates they measured varied between 1.6×10^{-6} and 1.5×10^{-8} mole/cm^2/s for 0–7 to 40–60 min., respectively (open circles in Fig. 3) and are lower than the rates observed in the current experiments despite the higher temperature in their runs. Nagahara and Ozawa (1996) and Tsuchiyama (1999) observed an increase in the evaporation rate of forsterite with increasing hydrogen pressure.

3.2. Low P and Low T Experiments

Following the results of experiments conducted at low P and high T, in which neither sulfide nor metallic metal was found, experiments on the survival of these components at lower T were conducted. Conditions in these experiments were set to 1350°C, hydrogen pressure of 1.31×10^{-5} atm and heating times of 2, 10 and 30 min. (Fig. 4). The charge produced by 2 min. heating (Fig. 4a) contains large metal-sulfide blebs, especially on or near the charge surface. The troilite is the host phase of these blebs and it contains large cellular-dendritic kamacite crystals plus pores. Figure 5 shows BSE images of three different regions on the surface of this charge, with different sulfide-metal ratios. The troilite occurs as feathery dendritic crystals grown on the quench, in the sulfide-rich metal-poor regions (Fig. 5a). In more metal-rich areas, surface kamacite grains have a bowl shape, in some cases containing residual sulfide puddles (Fig. 5b). Where they are empty, the kamacite bowls have etched or terraced interiors (Fig. 5c) similar to those produced by Tsuchiyama and Fujimoto (1995).

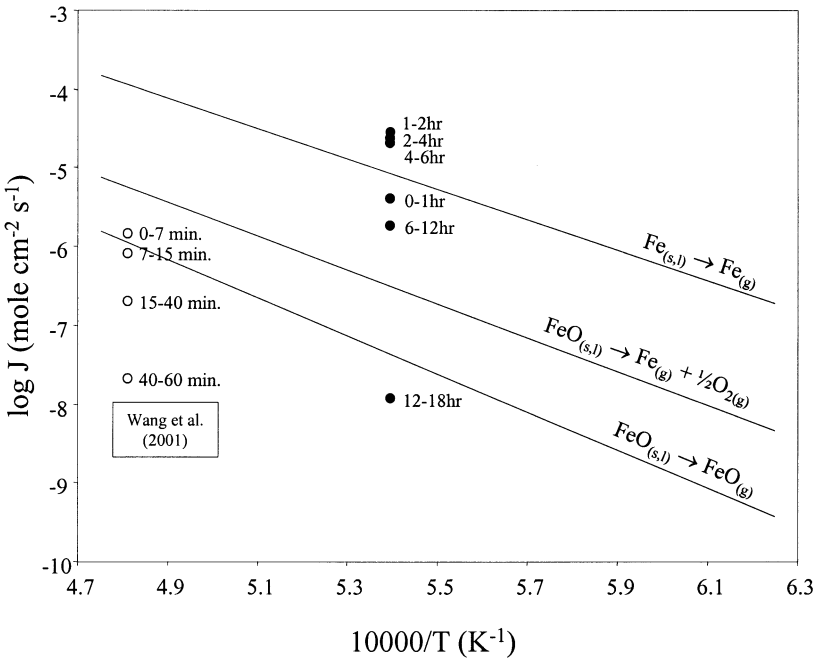

Fig. 3. Arrhenius relation of the evaporation of FeO and Fe-metal for several reactions involving pure phases modified after Wang et al. (1994), calculated using thermochemical data from Barin (1989). The results from our low pressure experiments fall above the $FeO \rightarrow Fe_{(g)} + \frac{1}{2}O_{2(g)}$ and are marked by the solid circles. Results from similar experiments, performed in air by Wang et al. (2001), are shown as open circles.

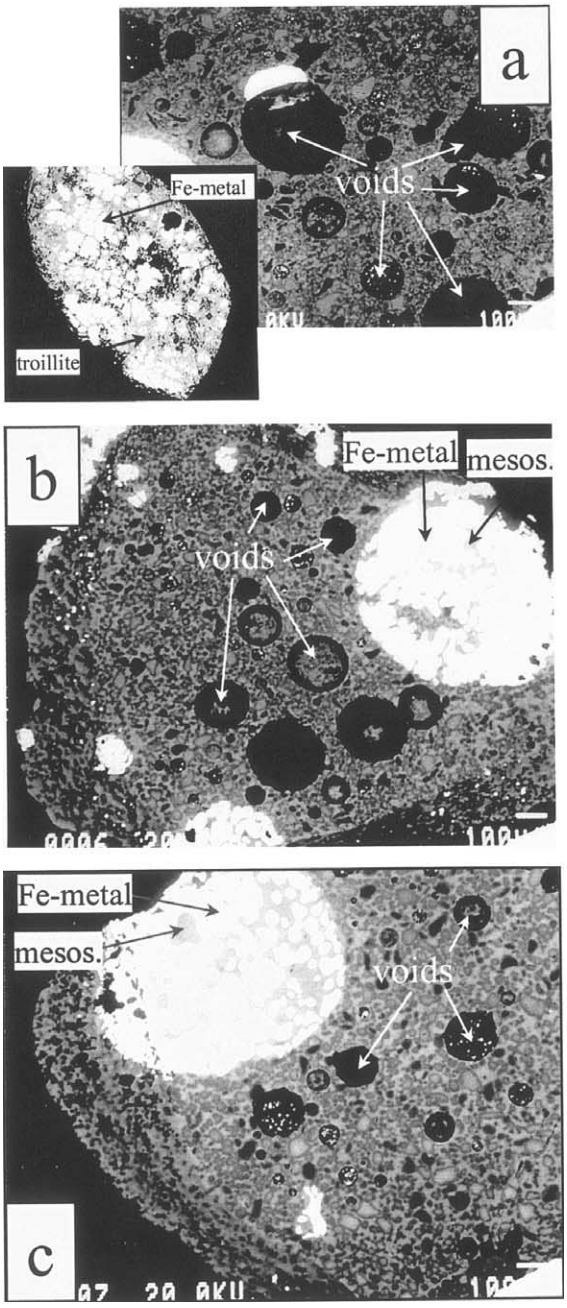

Fig. 4. Cross sections through charges produced at 1.3×10^{-5} atm and 1350°C. (a) 2 min run. (b) 10-min run. (c) 30-min run. Metal dendrites have grown in sulfide melt with voids (a) which is later replaced by silicate melt (b, c). The presence of vesicles is due to the low degree of melting. The apparent porous rinds on the charges are due to unpolished material lying below the epoxy.

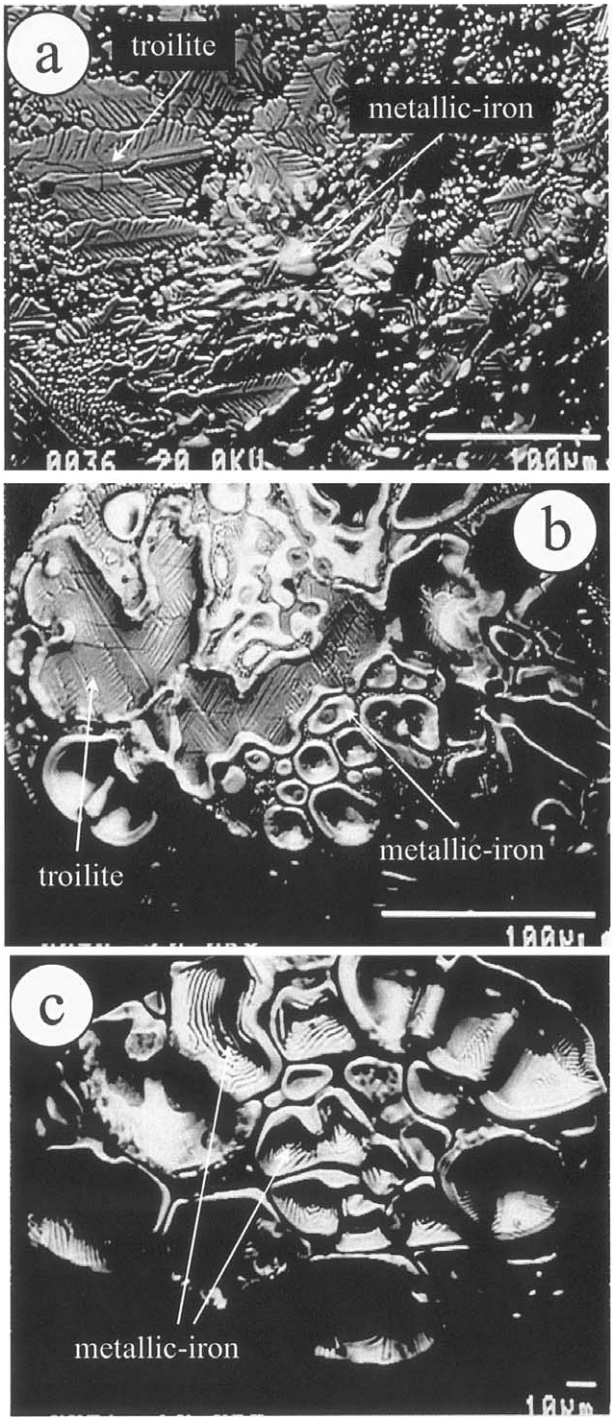

Fig. 5. Back scattered electron images of 3 different areas on the surface of the 2-min charged produced at 1.31×10^{-7} atm, fO_2 of IW-4.8 and 1350°C. The images represent different stages in the desulfurization process of troilite.

The charges produced by 10 and 30 min. heating contain iron metal but no sulfide. The kamacite is globular-dendritic and set in silicate glass (Figs. 4b,c), the two phases being pseudomorphous after sulfide blebs. The metal in these charges exhibits a slight decrease in the amount of iron and a similar increase in the amount of nickel between the 10 min and the 30 min runs (Table 3). These changes are expected as elements such as sulfur and copper evaporate from the metal (Zanda et al., 2002). The occurrence of nickel in the metal phase is associated with the partial melting of the starting material. Under highly reducing conditions nickel would migrate from the silicate phase to the metal.

The silicate portion in the 10 and 30-min charges contains vesicles and many relict grains, indicating very low degrees of

Table 3. Chemical composition (in wt%) of troilite and the metal phases from the low P and T experiments and of the pyrrhotite and the metal phases from the high P and T experiments. Analyses were performed on an electron probe.

Heating	Fe	S	Ni	Co	P	Cu	Total
			Low P and low T experiments				
Troilite	63.4	36.5	bd[a]	bd	bd	bd	99.9
2 min	97.67	0.059	0.126	0.203	0.004	0.133	98.19
10 min	98.49	0.011	0.182	0.189	0.007	0.014	98.89
30 min	98.02	0.009	0.202	0.209	0.014	0.039	98.49
			High P and high T experiments				
Pyrrhotite	61.8	38.3	bd	bd	bd	bd	100.1
1 h	97.22	bd	1.007	0.193	0.432	0.003	98.86
2 h	98.06	bd	1.274	0.169	0.492	0.017	100.01
4 h	96.82	bd	1.097	0.168	0.517	0.000	98.60
6 h	96.78	bd	1.174	0.198	0.598	0.006	98.75

[a] bd = below detection.

melting. The relict grains have reverse zoning, indicating dissolution of the fayalite component into the melt. These types of textures, clast-laden melts and metal-glass intergrowths, are rare to nonexistent in natural chondrules, which for the most part did not experience evaporation at low degrees of melting (Hewins and Radomsky, 1990).

3.3. High P and High T Experiments

Back scattered electron images of the experimental charges, heated for 1, 2, 4, 6, 12 and 18 h at 1 atm, in H_2-CO_2, fO_2 of IW-3 and 1565°C, are presented in Figure 6. These charges consist of olivine grains, mesostasis and iron metal. Olivine grains vary in size. They are smaller in the shorter runs (10–20μm) and tend to be larger in the long-heating runs (up to 100μm).

Metallic iron appears in two forms. The first consists of round blebs present in the charges heated for 1, 2, 4 and 6 h and contains various amounts of sulfur, nickel and phosphorus (Table 3). These iron blebs are a few microns in size (Fig. 6a), but rapidly coagulate to form large metal globules of up to 1 mm across (Figs. 6a–d). In longer runs a decrease in the globule sizes is observed (Fig. 6d) and charges heated for 12 and 18 h (Figs. 6e,f) do not contain any. These forms of metallic iron resemble the iron metal found for example in Renazzo chondrules. Figures 7a,b compares a chondrule and a charge with many small metal droplets, and Figures 7c,d a chondrule and a charge with a very large metal globule. The compositions of this form of metal are shown in Table 3. The metal compositions consist mostly of iron with ~1 wt% nickel and traces of cobalt and phosphor. The higher content of nickel in these experiments relative to the high P low T is attributed to the higher temperature, leading to higher degrees of melting. The increases in Ni and P are consistent with observations by Connolly et al. (2001) and Zanda et al. (2002). Zanda et al. (2002) suggested that the unexpectedly elevated concentration of P in the metal is related to oxidation of Fe at the interface between the metal and the surrounding silicate melt.

The second form of metallic-iron is observed in olivine grains as dusty cores, white in BSE, similar to the known dusty olivines in chondrules (Nagahara, 1981; Grossman et al., 1988; Jones and Danielson, 1997). In Figures 7d,e we show the similar development of dusty olivine in our charges to olivine grains in a chondrule from Semarkona. Dusty olivines exist in all our charges even those heated for 12 and 18 h. In some of the charges metal grains occur as linear arrays in the olivine crystals (Fig. 7e). Such a display was observed in natural chondrules as well and was interpreted by Jones and Danielson (1997) as possible nucleation and growth of iron along preferred crystallographic directions in olivine during a reduction process. Boland and Duba (1981) and Lemelle et al. (2000) also produced this effect during experimental reduction of olivine.

The chemical compositions of the olivine and the mesostasis from the different charges are shown in Table 4. The Fo content in the olivine increases rapidly, from a nominal 70% in the unheated starting composition to ~97–98% in the 1–2-h runs and to ~99% in the 4–18-h ones. The iron loss from the olivine after only 1 h in 1 atm is greater than the loss in the first 6 h at low pressure. The loss of FeO from the mesostasis at 1 atm is faster as well, for example after 1 h the mesostasis contains 4.01 wt% FeO in the 1-atm run compared to 25.95 wt% at the low pressure.

The concentrations of CaO, Al_2O_3 and TiO_2 in the mesostasis increased dramatically from 1 h to 6 h, to the levels reached in 12 and 18 h at low pressure, indicating either crystallization of olivine or evaporation (Table 4). However, FeO, SiO_2 and MgO show a gradual decrease, which is in agreement with an evaporative process rather than crystallization (or dissolution) of olivine. After 6 h of evaporation, the composition trends reverse, with refractory elements decreasing and MgO increasing in the melt, indicating dissolution of olivine. Silica, however, continues to decrease. Evidence for the dissolution of olivine is observed in the charges of 12 and 18-h runs (Figs. 6e,f), in which the olivine content is lower relative to the previous runs. Massive evaporation of FeO increases the relative abundance of SiO_2 in the melt, which causes the dissolution of olivine grains. Olivine dissolution would increase the concentration of MgO, decrease the SiO_2, and dilute the CaO, Al_2O_3 and TiO_2 in the melt of the 12 and 18-h runs (Table 4).

As in the low-pressure experiments, the manner in which FeO was lost can be confirmed by comparison with the MnO content. The concentrations of FeO and MnO in the olivine

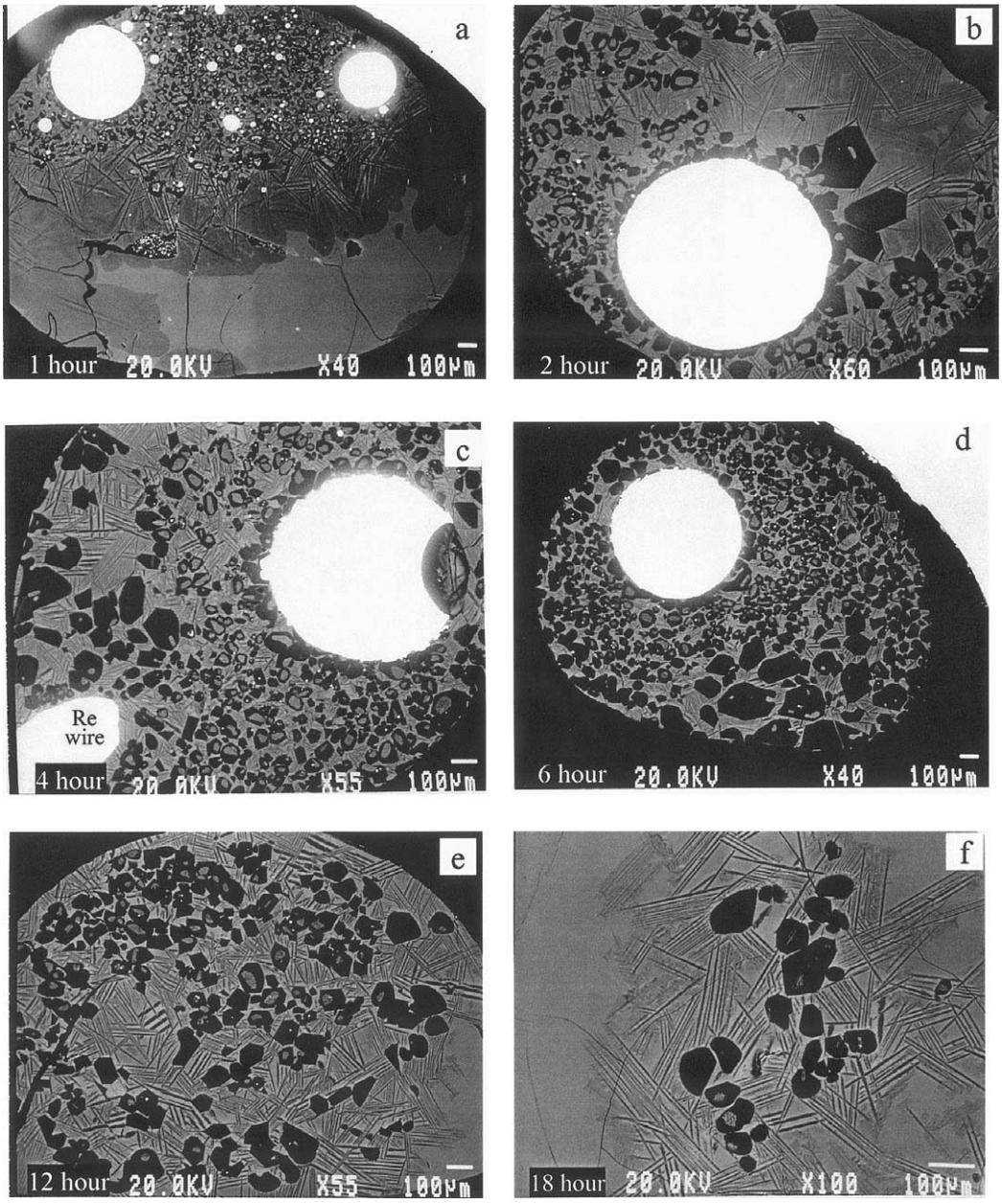

Fig. 6. Back-scattered electron images of experimental charges produced at 1 atm, fO_2 of IW-3 and 1565°C. They contain Fe-metal blebs, olivine grains with or without "dusty" cores, mesostasis and olivine quench dendrites. Each image (a–f) represents a different heating time (1–18 h).

grains and in the mesostasis in the experimental charges display a similar decrease with increasing heating times (Fig. 8) implying, as in the low-pressure experiments, that FeO was lost due to evaporation, by way of hydrogen stripping. As was noted earlier inferring the fashion in which FeO was lost by comparison with MnO content is feasible only if the reduction rate of FeO is different than the evaporation rate of MnO. The likelihood that these rates are comparable in both sets of experiments (each conducted at different T, P and P_{H2}) and in both phases (olivine and glass) is highly unlikely.

The Fo and CaO (wt%) contents of the olivine in the charges from the low-pressure experiments, the 1-atm experiments and natural chondrules are presented in Figure 9. It is noticeable that the olivines produced in 1-atm experiments after only 1 h of evaporation have Fo and CaO contents produced after at least 6 h of evaporation at low H_2-pressures. Within 4 h of evaporation the olivines have compositions of Fo_{99}. Similar olivine compositions require 12 h to form at lower H_2-pressures.

The more rapid increase in the Fo content of the olivines and the faster loss of FeO from the mesostasis in the 1-atm experiments might be expected if reduction of Fe were the principle mechanism for FeO removal. However, in that case MnO and FeO should not decrease together as they do in Figure 8. With a higher hydrogen pressure, more hydrogen molecules are

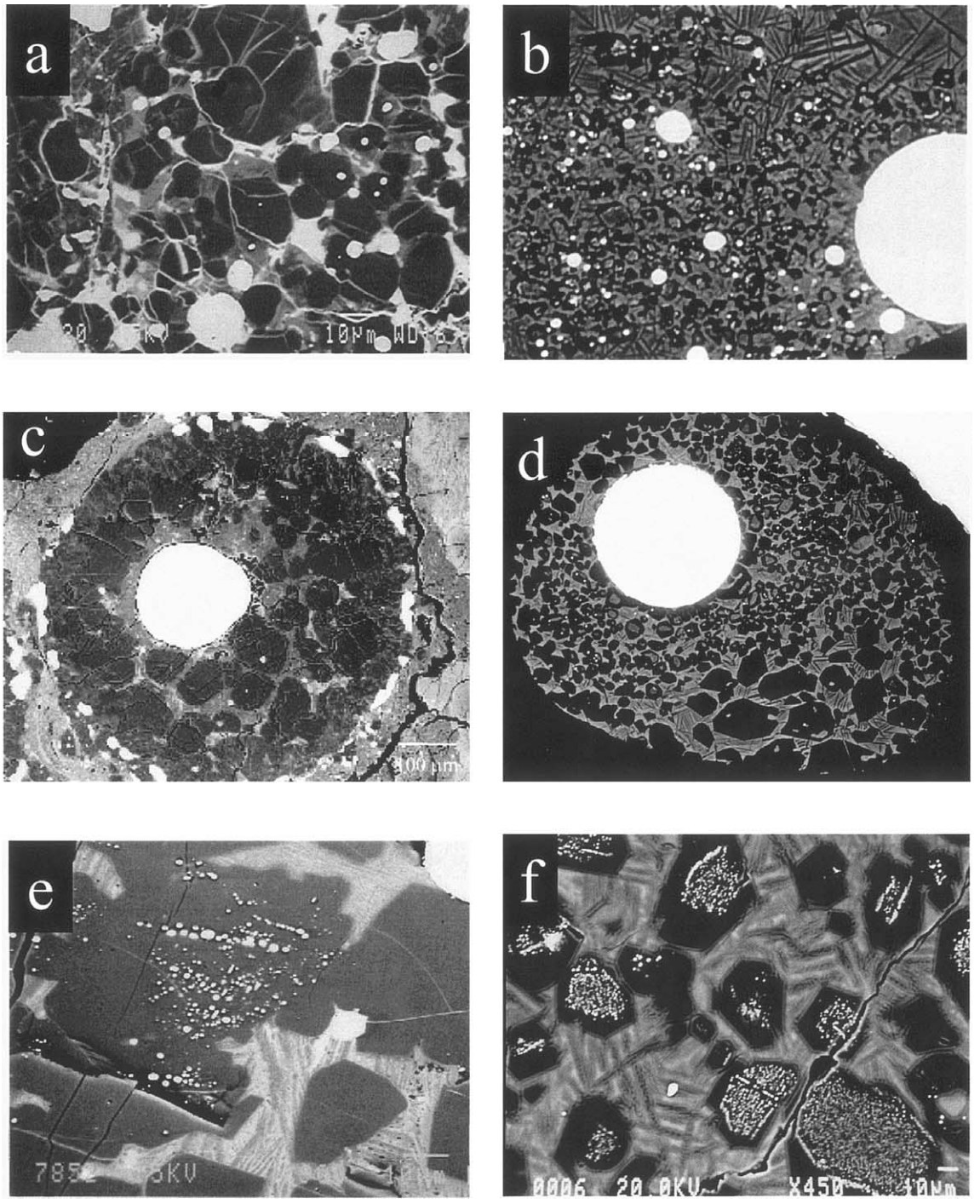

Fig. 7. Limited degree of coalescence of small metallic blebs in a Renazzo chondrule (a) and in a 1-h charge run at 1-atm H_2 (b). A large metal bleb at the center of a Renazzo chondrule with smaller blebs surrounding the rim (c), similar to a large metal bleb in the center of a 6-h charge produced at 1-atm H_2 (d). Dusty olivine in a Semarkona chondrule (e) and in a 1-h charge produced at 1-atm H_2 (f).

available for stripping oxygen coordinated to volatiles such as Fe, Mn and Na and we conclude that hydrogen stripping, and not reduction, is the dominant process responsible for FeO loss. The fact that most FeO was lost due to evaporation rather than reduction has extreme importance when interpreting the origin of the iron metal, which is so pervasive in these charges.

4. DISCUSSION

4.1. Origin of Iron Metal Blebs in the Experimental Charges

In low-pressure (1.31×10^{-5} atm) and high temperature (1580°C) experiments, the compositions and textures of Type

Table 4. Chemical compositions of olivine and mesostasis (in wt%) produced at 1-atm H_2-CO_2 and 1565°C. Analyses were performed on an electron probe.

Oxide (wt%)	1 h	s.d.[a]	2 h	4 h	6 h	12 h	18 h
Olivine							
No. of analyses	12		23	29	11	10	20
SiO_2	42.47	0.43	42.56	42.90	42.56	42.64	42.78
Al_2O_3	0.005	0.084	0.01	0.07	0.03	0.16	0.16
TiO_2	0.01	0.009	0.01	0.01	0.01	0.01	0.02
FeO	2.62	0.64	1.78	0.71	0.71	0.37	0.33
MnO	0.09	0.021	0.05	0.02	0.015	0.006	0.003
MgO	55.93	0.40	56.66	57.32	57.53	57.39	57.41
CaO	0.08	0.083	0.10	0.18	0.20	0.42	0.43
Fo content	97.44		98.28	99.30	99.31	99.64	99.68
Mesostasis							
No. of analyses	7		9	5	12	10	8
SiO_2	53.35	0.43	52.25	49.80	43.39	40.21	41.30
Al_2O_3	4.52	0.53	7.27	12.64	18.21	17.44	16.06
TiO_2	0.10	0.018	0.16	0.32	0.41	0.37	0.32
FeO	4.01	0.10	1.58	1.05	0.72	0.37	0.43
MnO	0.18	0.008	0.05	0.04	0.005	0.001	0.002
MgO	34.74	1.16	33.54	24.45	21.63	28.11	30.45
CaO	3.70	0.50	6.25	12.38	16.02	14.05	12.12
Result	Evaporation		Evaporation	Evaporation	Evaporation	Olivine dissolution	Olivine dissolution

[a] Averaged standard deviations.

IA and IIA chondrules were produced, but iron metal blebs and dusty olivines were not formed despite favorable conditions (20 wt% troilite in their starting material). In these experiments Fe-metal was clearly lost by evaporation.

In the low pressure (1.31×10^{-5} atm) and low temperature runs (1350°C), Fe-metal was observed to have formed by sulfur loss from a FeS melt (desulfurization). While these charges do not resemble natural chondrules, because of numerous relict olivine grains and olivine dendrites with interstitial silicate glass, they provide an insight into the stability of sulfide melt at relatively low temperatures. At 1350°C sulfur in FeS melt was retained for less than 10 min. and was lost much faster than iron metal. These experiments clearly show that the iron metal was produced by gradual sulfur loss (Fig. 4). Low temperature experiments also demonstrate that the presence of either Fe-Ni sulfide or Fe-Ni metal in the precursor of chondrules is indistinguishable as far as the end product is concerned. This is because after sulfur is lost from sulfide melt, metal remains. As chondrule formation occurred at temperature well above 1350°C, no evidence of the former presence of sulfide is expected, unless high ambient pressures of sulfur were present.

In charges produced at 1-atm H_2-CO_2 and 1565°C iron metal was pervasive. This metal might have been produced in several ways. One possibility is that it formed by the reduction of FeO while moderately volatile lithophile elements are retained in the melt. Tsuchiyama and Miyamoto (1984) produced metal blebs on the surface of charges by reduction in a CO-CO_2 mixture at an oxygen fugacity of IW-1.5. Under similar conditions, Na loss from the melt is relatively slow (Yu and Hewins, 1998) and Mn loss is minimal. However, in our experiments Na loss is complete, and Mn loss extensive. In addition MnO and FeO are correlated both in the olivine grains and the mesostasis, which supports FeO evaporation rather than reduction to Fe-metal.

An alternative source for the iron metal is the desulfurization of FeS similar to the results observed in the low T low P

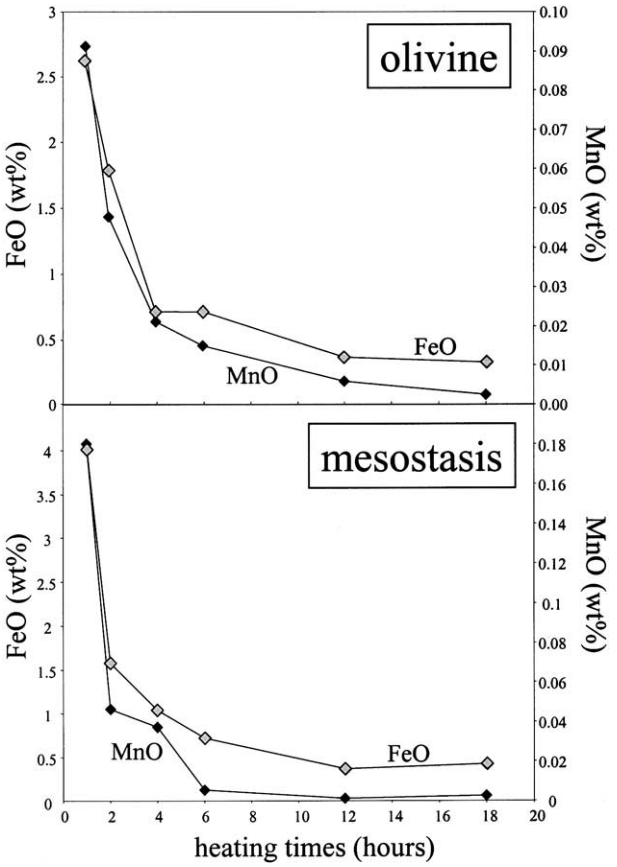

Fig. 8. FeO (wt%) and MnO (wt%) in the olivine grains of 1-atm experiments and in the mesostasis of 1-atm experiments.

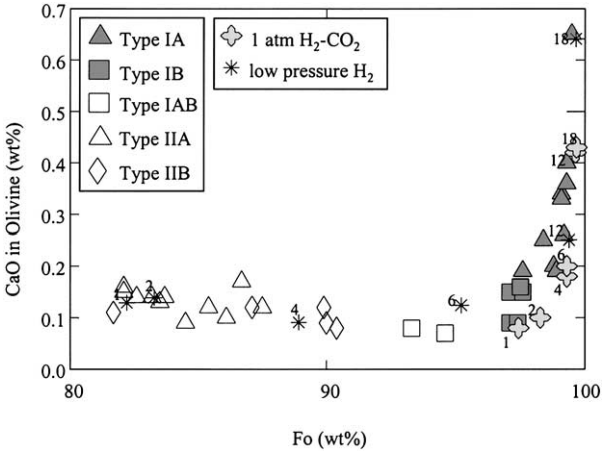

Fig. 9. CaO content in olivine in wt% vs. the Fo content in olivine, in Semarkona chondrules (Jones and Scott, 1989; Jones, 1990, 1994, 1996) and in evaporation residues from low pressure and 1-atm experiments.

experiments. At the experimental temperature, 1565°C, sulfur is highly volatile but iron metal is much less so. Sulfur loss by hydrogen-reduction leaves liquid metallic-iron, the external pressure exceeding the vapor pressure of iron, as in the reaction proposed by Tachibana and Tsuchiyama (1998):

$$FeS_{(s,l)} + 1/2H_2 \rightarrow Fe^{o}_{(l)} + HS_{(g)} \quad (4)$$

This interpretation of our experimental results is consistent with observations of natural chondrules where texture-composition correlations suggest desulfurization during chondrule formation (Hewins et al., 1997) and where some iron-metal is equilibrated with the hosting silicates (Zanda et al., 1994).

The experiments conducted at 1-atm hydrogen produced Type I chondrule bulk compositions and, because of S loss, the typical metallic iron found in chondrules. These results suggest higher than canonical pressures for chondrule formation. The minimum pressure needed for maintaining Fe-metal in the melt can not be inferred from the present study. In general our experiments demonstrate the various effects of hydrogen pressures on reactions such as hydrogen stripping and desulfurization. In low hydrogen pressure runs, FeO in silicates lasted longer and Fe-metal evaporated immediately. Conversely, at 1-atm hydrogen, FeO in silicates was lost faster while Fe-metal remained in the melt for over 12 h.

4.2. Origin of Dusty Olivine in the Experimental Charges

Olivine with Fe-metal inclusions has been produced using either graphite, as a crucible or incorporated in the starting material, or reducing gasses (Boland and Duba, 1981; Connolly et al., 1994; Danielson and Jones, 1995; Libourel and Chaussidon, 1995; Lemelle et al., 2000). It has been suggested that at high temperatures dusty olivine be formed by the reduction of Fe^{+2} in olivine, as in the reaction (Libourel and Chaussidon, 1995):

$$\text{olivine } (Fo_{70}) \rightarrow \text{olivine } (Fo_{>70}) + \text{Si-rich melt} + \text{Fe-metal} + O_2 \quad (5)$$

The evaporation of the Fe derived from sulfide melt into the vapor suggests that gas did not create the metal inclusions in our olivine. We therefore suggest that the kerogen, present in the starting material, reduced the iron in the olivine to make dusty olivine. This occurred within the first hour of heating while the kerogen material was still present. In experiments of longer heating times (2–18 h) newly grown olivine, either as mantles surrounding old olivine cores or as newly grown crystals, are clear of metal inclusions (Fig. 6). The lack of metal inclusions in these grains is attributed to the nearly complete loss of FeO from the olivine grains within the first hour and to the evaporative nature of kerogen.

4.3. Origin of Iron Metal in Chondrules

Though some chondrules may have formed by direct condensation, we consider here the model of reheating of precursor solid aggregates to produce chondrules. The occurrence of Fe-metal in Type I chondrules could be related to the evaporation and/or reduction of a low temperature precursor resembling CI or Type II chondrules. The occurrence of iron in the precursors of chondrules may have been in the form of Fe-silicate, Fe-sulfide or Fe-metal grains, whether they originated as circumstellar or nebular condensates. The presence of S in many chondrules and the equilibrium low temperature assemblage given by condensation sequences (Grossman, 1972; Wood and Hashimoto, 1993; Ebel and Grossman, 1997, 2000) indicate that the presence of Fe-metal in the chondrule precursors was rather unlikely. In our low T and low P experiments FeS becomes Fe-metal within minutes. Thus experiments with sulfide are virtually identical to experiments with Fe in the precursors.

Many have suggested that Fe-metal in chondrules is the product of the reduction of Fe silicate (Scott and Taylor, 1983; Johnson, 1986; Lee et al., 1992; Kong and Palme, 1999; Connolly et al., 2001) by either carbon in the chondrule precursors (Connolly et al., 1994; Connolly et al., 2001) or by hydrogen (Sears et al., 1996). Others have proposed sulfur loss (desulfurization) from FeS as the generator of significant amounts of metallic iron in chondrules (Zanda et al., 1994).

Experiments conducted under canonical nebular conditions did not produce iron metal, despite the presence of two potentially reducing agents, kerogen and hydrogen. Kerogen, which could have potentially generated iron metal by reduction of Fe silicates, is extremely volatile and was lost before substantial reduction took place. Hydrogen at low pressure is clearly effective at removing O and associated Na, Fe, etc., from the melt and does not reduce FeO and leave Fe-metal behind. Iron sulfide is also a potential source for iron metal as a result of S loss, but Fe° is extremely volatile under these conditions, the equilibrium vapor pressure exceeding the total pressure.

Although experiments conducted at lower temperature (i.e., 1350°C) produced iron metal and sulfides, the textures exhibited by these charges are not characteristic of natural chondrules. The experiment temperature was far below the liquidus of the silicate precursors, which left a myriad of relict grains

and vesicles. The metal produced in these experiments does not resemble that in natural chondrules either (e.g., McSween, 1977; Jones and Scott, 1989) nor do the evaporation textures of solid metal "dendrites" (Figs. 4 and 5). Most Type I chondrules, whether melted extensively or to a low degree, contain drop-formed metal. They were therefore heated to at least 1500°C for variable amounts of time.

The experiments conducted at 1-atm in H_2-CO_2 produced various types of iron-metal found in natural chondrules, i.e., metal iron blebs and dusty olivine. Elevated hydrogen pressure was evidently extremely important in both allowing the desulfurization of FeS and suppressing the evaporation of Fe-metal from the melt.

Chondrules were not produced by a simple one-stage process like the isothermal evaporation of our experiment. They probably experienced melting and evaporation followed by crystallization and condensation during cooling. The iron metal, which typically surrounds the rims of chondrules (as seen in Fig. 7c), may be explained in a similar way. This type of metal contains lower Ni and Co concentrations relative to the interior metal blebs (Lee et al., 1992), and probably formed by recondensation during cooling of chondrules (Connolly et al., 2001; Zanda et al., 2002).

However to keep iron-metal in chondrules during their formation, pressures in the chondrule formation region had to have been higher than canonical, as demonstrated by our experiments. High partial pressures of volatile elements relative to the solar nebula appear necessary for the retention of volatile elements in the silicate melt, especially during the formation of Type II chondrules (Yu et al., 2003 and Yu and Hewins, 1998). Experiments have shown that iron sulfide can be retained in a melt for as long as 4 h due to high partial pressures of iron and sulfur surrounding the melt (McCoy et al., 1999). However, it is not clear whether high partial pressures of volatile elements would have helped retain iron-metal in chondrules, as iron metal is most abundant in those that lack volatile elements (i.e., Type I chondrules): the gas would have to be enriched in Fe but depleted in Na.

Our results suggest that the occurrence of iron metal in Type I chondrules requires higher total pressure than those of the canonical nebula. Formation in a transient asteroidal or planetary atmosphere has been suggested but is not well established (Grossman, 1988). If chondrules are nebular in origin, a special environment in the solar nebular needs to be sought. The proposition that chondrule formation occurred at ambient pressures higher than canonical has been raised in several studies (Hood and Horanyi, 1993; Connolly and Love, 1998). Chondrules and their surrounding gas were conceivably compressed during the passage of a shock wave. These pressures probably reached $\sim 10^{-3}$ atm for a minimum mass nebula (Desch, personal communication). Others like Galy et al. (2000), in an effort to explain Mg-isotopic compositions in chondrules, proposed that chondrules formed in the solar nebula at higher than 10^{-3} atm. The vapor pressure of Fe at the temperatures of interest is $\sim 10^{-4}$ bars, so the presence of metal suggests a higher pressure. Further experiments are obviously necessary to determine the minimum pressure needed for maintaining iron metal in the melt.

5. SUMMARY

A CI analog heated at chondrule melting temperatures under canonical nebular conditions produced evaporation residues lacking iron metal, due to the high volatility of FeS and iron-metal at these conditions. The presence of hydrogen was shown to be effective in enhancing the evaporation of FeO, rather than in reducing it to liquid metal.

At low peak temperatures (i.e., 1350°C) and low hydrogen pressure sulfide and iron metal survived only with short heating times. The abundant relict olivine grains and metal-sulfide evaporation textures of these experiments are typically absent in chondrules, indicating different conditions. The droplet textures of metal in Type I chondrules require at least 1500°C.

Experiments conducted in H_2-CO_2 at 1-atm, produced Fe-metal blebs and dusty olivines, similar to those observed in natural chondrules. The majority of metallic iron blebs (small and large) are believed to have formed by sulfur loss within the first hour of the experiment. We estimate that the only metal grains formed by reduction of silicate were the iron inclusions in olivine grains (dusty olivine), produced by kerogen reduction within the first hour of evaporation.

The melts produced in these experiments exhibited evaporative losses of FeO and SiO_2. In the 1-atm experiments the evaporation of FeO is faster and that of Fe-metal is slower than in the low-pressure (canonical nebula) experiments.

Higher total pressures relative to the canonical nebula may have been necessary for allowing metallic iron to survive at chondrule peak temperatures. Elevated partial pressures of certain elements (such as Fe) due to dust evaporation in the ambient gas may have contributed as well.

Acknowledgments—We thank Yang Yu, Brigitte Zanda and Jeremy Delaney for discussion and important insights, Mike Carr for the DCP work and the Muséum National d'Histoire Naturelle in Paris for supplying materials for this study. Reviews by Jeff Grossman and an anonymous reviewer have improved the manuscript significantly. This work was supported by NASA grants NAG5-4472, NAG5-4579 and NAG5-10494.

Associate editor: C. Koeberl

REFERENCES

Anders E. and Grevesse N. (1989) Abundance of the elements: Meteoritic and solar. *Geochim. Cosmochim. Acta.* **53,** 197–214.

Barin I. (1989) *Thermodynamical Data of Pure Substances*. VHC.

Boland J. N. and Duba A. (1981) Solid-state reduction of iron in olivine—Planetary and meteoritic evolution. *Nature* **294,** 142–144.

Cohen B. A., Hewins R. H., and Yu Y. (2000) The formation of chondrules by open-system melting of nebular condensates Evaporation in the young solar nebula as the origin of "just-right" melting of chondrules. *Nature* **406,** 600–602.

Connolly H. C., Jr., Hewins R. H., Ash R. D., Zanda B., Lofgren G. E., and Bourot-Denise M. (1994) Carbon and the formation of reduced chondrules: An experimental investigation. *Nature* **371,** 136–139.

Connolly H. C., Jr. and Love S. G. (1998) The formation of chondrules: Petrologic tests of the shock wave model. *Science* **280,** 62–67.

Connolly H. C., Jr., Huss G. R., and Wasserburg G. J. (2001) On the formation of Fe-Ni metal in Renazzo-like carbonaceous chondrites. *Geochim. Cosmochim. Acta.* **65,** 4567–4588.

Danielson L. R. and Jones R. H. (1995) Experimental reduction of olivine: Formation of dusty relict olivine in chondrules (abstract). *Lunar Planet. Sci.* **26,** 309–310.

Darken L. S. and Gurry R. W. (1945) The system iron-oxygen. I. The

wüstite field and related equilibria. *J. American Chem. Soc.* **67,** 1398–1412.

Deines P., Nafziger R. H., Ulmer G. C., and Woermann E. (1974) *Temperature-Oxygen Fugacity Tables for Selected Gas Mixtures in the System C-H-O at One Atmosphere Total Pressure*. Pennsylvania State University.

Ebel D. S. and Grossman L. (1997) Direct condensation of ferromagnesian liquids from cosmic gases (abstract). *Lunar Planet. Sci.* **28,** 317–318.

Ebel D. S. and Grossman L. (2000) Condensation in dust-enriched systems. *Geochim. Cosmochim. Acta.* **64,** 339–366.

Eugster H. P. and Wones D. R. (1962) Stability relations of the ferruginous biotite, annite. *J. Petrol* **3,** 81–124.

Galy A., Young E. D., Ash R. D., and O'Nions R. K. (2000) The formation of chondrules at high gas pressures in the solar nebula. *Science* **290,** 1751–1753.

Grossman L. (1972) Condensation in the primitive solar nebula. *Geochim. Cosmochim. Acta.* **36,** 597–617.

Grossman J. N. (1988) Formation of chondrules. In *Meteorites and the Early Solar System* (eds. J. F. Kerridge and M. S. Matthews), pp. 680–696. University of Arizona.

Grossman J. N. (1996) Chemical fractionation of chondrites: Signatures of events before chondrule formation. In *Chondrules and the Protoplanetary Disk* (eds. R. H. Hewins, R. H. Jones, and E. R. D. Scott), pp. 243–253. Cambridge University Press.

Grossman J. N. and Wasson J. T. (1985) The origin and history of the metal and sulfide components of chondrules. *Geochim. Cosmochim. Acta.* **49,** 925–939.

Grossman J. N., Rubin A. E., Nagahara N., and King E. A. (1988) Properties of chondrules. In *Meteorites and the Early Solar System* (eds. J. F. Kerridge and M. S. Matthews), pp. 680–696. University of Arizona.

Haack H. and Scott E. R. D. (1993) Nebula formation of the H, L, and LL parent bodies from a single batch of chondritic materials (abstract). *Meteoritics* **28,** 358–359.

Herzberg C. T. (1979) The solubility of olivine in basaltic liquids: An ionic model. *Geochim. Cosmochim. Acta.* **43,** 1241–1251.

Hewins R. H. and Radomsky P. M. (1990) Temperature and conditions for chondrule formation. *Meteoritics* **25,** 309–318.

Hewins R. H., Yu Y., Zanda B., and Bourot-Denise M. (1997) Do nebular fractionation, evaporative losses, or both, influence chondrule compositions? *Antarct. Meteorite Res.* **10,** 275–298.

Hood L. L. and Horanyi M. (1993) The nebular shock wave model for chondrule formation: One-dimensional calculation. *Icarus* **106,** 179–189.

Huebner J. S. (1987) Use of gas mixtures at low pressure to specify oxygen and other fugacities of furnace atmospheres. In *Hydrothermal Experimental Techniques* (eds. G. C. Ulmer and H. L. Barnes), pp. 20–60. Wiley.

Johnson M. C. (1986) The solar nebula redox state as recorded by the most reduced chondrules of five primitive chondrites. *Geochim. Cosmochim. Acta.* **50,** 1497–1502.

Jones R. H. (1990) Petrology and mineralogy of Type II, FeO-rich chondrules in Semarkona (LL3.0): Origin by closed-system fractional crystallization, with evidence for supercooling. *Geochim. Cosmochim. Acta.* **54,** 1785–1802.

Jones R. H. (1994) Petrology of FeO-poor, porphyritic pyroxene chondrules in the Semarkona chondrite. *Geochim. Cosmochim. Acta.* **58,** 5325–5340.

Jones R. H. (1996) FeO-rich porphyritic pyroxene chondrules in unequilibrated ordinary chondrites. *Geochim. Cosmochim. Acta.* **60,** 3115–3138.

Jones R. H. and Danielson L. R. (1997) A chondrule origin for dusty relict olivine in unequilibrated chondrites. *Meteorit. Planet. Sci.* **32,** 753–760.

Jones R. H. and Scott E. R. D. (1989) Petrology and thermal history of Type IA chondrules in Semarkona (LL3.0) (abstract). *Proc. Lunar Planet. Sci. Conf.* **19,** 523–536.

Kong P. and Palme H. (1999) Compositional and genetic relationship between chondrules, chondrule rims, metal and matrix in the Renazzo chondrite. *Geochim. Cosmochim. Acta.* **63,** 3673–3682.

Krot A. N., Meibom A., Petaev M. I., Keil K., Zolensky M. E., Saito A., Mukai M., and Ohsumi K. (2000) Ferrous silicate spherules with euhedral iron-nickel metal grains from CH carbonaceous chondrites: Evidence for supercooling and condensation under oxidizing conditions. *Meteorit. Planet. Sci.* **35,** 1249–1258.

Larimer J. W. and Wasson J. T. (1988) Siderophile element fractionation. In *Meteorites and the Early Solar System* (eds. J. F. Kerridge and M. S. Matthews), pp. 416–435. University of Arizona.

Lee M. S., Rubin A. E., and Wasson J. T. (1992) Origin of metallic Fe-Ni Renazzo and related chondrites. *Geochim. Cosmochim. Acta.* **56,** 2521–2533.

Lemelle L., Guyot F., Fialin M., and Pargamin J. (2000) Experimental study of chemical coupling between reduction and volatilization in olivine single crystals. *Geochim. Cosmochim. Acta.* **64,** 3237–3249.

Libourel G. and Chaussidon M. (1995) Experimental constraints on chondrule reduction (abstract). *Meteoritics* **30,** 536–537.

McCoy T. J., Dickinson T. L., and Lofgren G. E. (1999) Partial melting of the Indarch (EH4) meteorite: A textural, chemical, and phase relations view of melting and melt migration. *Meteorit. Planet. Sci.* **34,** 735–746.

McSween H. Y. (1977) Chemical and petrographic constraints on the origin of chondrules and inclusions in carbonaceous chondrites. *Geochim. Cosmochim. Acta.* **41,** 1843–1860.

Nafziger R. H., Ulmer G. C., and Woerman E. (1971) Gaseous buffering for control of oxygen fugacity at one atmosphere. In *Research Techniques for High Pressure and High Temperature* (ed. G. C. Ulmer), pp. 9–41. Springer-Verlag.

Nagahara H. (1981) Evidence for secondary origin of chondrules. *Nature* **292,** 135–136.

Nagahara H. and Ozawa K. (1996) Evaporation of forsterite in H_2 gas. *Geochim. Cosmochim. Acta.* **60,** 1445–1459.

Rambaldi E. R. (1981) Relict grains in chondrules. *Nature* **293,** 558–561.

Scott E. R. D. and Taylor G. J. (1983) Chondrules and other components in C, O, and E chondrites: Similarities in their properties and origins (abstract). *Proc. Lunar Planet. Sci. Conf.* **14,** B275–B286.

Scott E. R. D. and Haack H. (1993) Chemical fractionation in chondrites by aerodynamic sorting of chondritic materials (abstract). *Meteoritics* **28,** 434.

Scott E. R. D., Love S. G., and Krot A. N. (1996) Formation of chondrites and chondrules in the protoplanetary nebula. In *Chondrules and the Protoplanetary Disk* (eds. R. H. Hewins, R. H. Jones, and E. R. D. Scott), pp. 87–96. Cambridge University Press.

Sears D. W. G., Lu J., Benoit P. H., DeHart J. M., and Lofgren G. E. (1992) A compositional classification scheme for meteoritic chondrules. *Nature* **357,** 207–211.

Sears D. W. G., Huang S., and Benoit P. H. (1996) Open-system behavior during chondrule formation. In *Chondrules and the Protoplanetary Disk* (eds. R. H. Hewins, R. H. Jones, and E. R. D. Scott), pp. 221–231. Cambridge University Press.

Tachibana S. and Tsuchiyama A. (1998) Incongruent evaporation of troilite (FeS) in the primordial solar nebula: An experimental study. *Geochim. Cosmochim. Acta.* **62,** 2005–2022.

Tsuchiyama A. (1999) Evaporation of forsterite in the primordial solar nebula; rates and accompanied isotopic fractionation. *Geochim. Cosmochim. Acta.* **63,** 2451–2466.

Tsuchiyama A. and Miyamoto M. (1984) Metal grains in chondrules: An experimental study (abstract). *Lunar Planet. Sci.* **15,** 868–869.

Tsuchiyama A. Fujimoto S. (1995) Evaporation experiments on metallic iron in vacuum. In *8th Proc. National Institute of Polar Research. Symp. Antarct. Meteorites*, Tokyo, Japan, 205–213.

Wang J., Davis A. M., Clayton R. N., and Mayeda T. K. (1994) Kinetic isotopic fractionation during the evaporation of iron oxide from liquid state (abstract). *Lunar Planet. Sci.* **25,** 1459–1460.

Wang J., Davis A. M., Clayton R. N., Mayeda T. K., and Hashimoto A. (2001) Chemical and isotopic fractionation during evaporation of the FeO-MgO-SiO_2-CaO-Al_2O_3-TiO_2 rare earth element melt system. *Geochim. Cosmochim. Acta.* **65,** 479–494.

Wood J. A. and Hashimoto A. (1993) Mineral equilibrium in fractionated nebular systems. *Geochim. Cosmochim. Acta*. **57,** 2377–2388.

Yu Y. and Hewins R. H. (1998) Transient heating and chondrule formation: Evidence from sodium loss in flash heating simulation experiments. *Geochim. Cosmochim. Acta.* **62,** 159–172.

Yu Y., Hewins R. H., Alexander C. M. O'D. and Wang J. (2003) Experimental study of evaporation and isotopic mass fractionation of potassium in silicate melts. *Geochim. Cosmochim. Acta.* **67,** 773–786.

Zanda B., Hewins R. H., and Bourot-Denise M. (1993) Metal precursors and reduction in Renazzo chondrules (abstract). *Meteoritics* **28,** 466–467.

Zanda B., Bourot-Denise M., Perron C., and Hewins R. H. (1994) Origin and metamorphic redistribution of silicon, chromium and phosphorus in the metal of chondrites. *Science* **265,** 1846–1849.

Zanda B. Bourot-Denise M., Hewins R. H., Cohen B. A., Delaney J. S., Humayun M., and Campbell A. J. (2002) Accretion textures, iron evaporation and re-condensation in Renazzo chondrules (abstract). *Lunar Planet. Sci*. **33,** 1852.